*Mineralogical Magazine, February 2017, Vol. 81(1), pp. 1–14*

# Lucchesiite, $CaFe_3^{2+}Al_6(Si_6O_{18})(BO_3)_3(OH)_3O$, a new mineral species of the tourmaline supergroup

FERDINANDO BOSI[1,*], HENRIK SKOGBY[2], MARCO E. CIRIOTTI[3], PETR GADAS[4], MILAN NOVÁK[4], JAN CEMPÍREK[4], DALIBOR VŠIANSKÝ[4] AND JAN FILIP[5]

[1] Dipartimento di Scienze della Terra, Sapienza Università di Roma, Piazzale A. Moro, 5, I-00185 Rome, Italy
[2] Department of Geosciences, Swedish Museum of Natural History, Box 50007, SE-10405 Stockholm, Sweden
[3] Associazione Micromineralogica Italiana, via San Pietro 55, I-10073 Devesi-Ciriè, Torino, Italy
[4] Department of Geological Sciences, Faculty of Science, Masaryk University, Kotlářská 2, 611 37, Brno, Czech Republic
[5] Regional Centre of Advanced Technologies and Materials, Palacký University, Šlechtitelů 27, 783 71 Olomouc, Czech Republic

[*Received 04 September 2015; Accepted 01 December 2015; Associate Editor: Ian Graham*]

**ABSTRACT**

Lucchesiite, $CaFe_3^{2+}Al_6(Si_6O_{18})(BO_3)_3(OH)_3O$, is a new mineral of the tourmaline supergroup. It occurs in the Ratnapura District, Sri Lanka (6°35′N, 80°35′E), most probably from pegmatites and in Mirošov near Strážek, western Moravia, Czech Republic, (49°27′49.38″N, 16°9′54.34″E) in anatectic pegmatite contaminated by host calc-silicate rock. Crystals are black with a vitreous lustre, conchoidal fracture and grey streak. Lucchesiite has a Mohs hardness of ~7 and a calculated density of 3.209 g/cm$^3$ (Sri Lanka) to 3.243 g/cm$^3$ (Czech Republic). In plane-polarized light, lucchesiite is pleochroic (O = very dark brown and E = light brown) and uniaxial (–). Lucchesiite is rhombohedral, space group $R3m$, $a \approx 16.00$ Å, $c \approx 7.21$ Å, $V \approx 1599.9$ Å$^3$, $Z = 3$. The crystal structure of lucchesiite was refined to $R1 \approx 1.5\%$ using ~2000 unique reflections collected with Mo$K\alpha$ X-ray intensity data. Crystal-chemical analysis for the Sri Lanka (holotype) and Czech Republic (cotype) samples resulted in the empirical formulae, respectively: $^{X}(Ca_{0.69}Na_{0.30}K_{0.02})_{\Sigma1.01}{}^{Y}(Fe^{2+}_{1.44}Mg_{0.72}Al_{0.48}Ti^{4+}_{0.33}V^{3+}_{0.02}Mn_{0.01}Zn_{0.01})_{\Sigma3.00}{}^{Z}(Al_{4.74}Mg_{1.01}Fe^{3+}_{0.25})_{\Sigma6.00}[{}^{T}(Si_{5.85}Al_{0.15})_{\Sigma6.00}O_{18}](BO_3)_3{}^{V}(OH)_3{}^{W}[O_{0.69}F_{0.24}(OH)_{0.07}]_{\Sigma1.00}$ and $^{X}(Ca_{0.49}Na_{0.45}\square_{0.05}K_{0.01})_{\Sigma1.00}{}^{Y}(Fe^{2+}_{1.14}Fe^{3+}_{0.95}Mg_{0.42}Al_{0.37}Mn_{0.03}Ti^{4+}_{0.08}Zn_{0.01})_{\Sigma3.00}{}^{Z}(Al_{5.11}Fe^{3+}_{0.38}Mg_{0.52})_{\Sigma6.00}[{}^{T}(Si_{5.88}Al_{0.12})_{\Sigma6.00}O_{18}](BO_3)_3{}^{V}[(OH)_{2.66}O_{0.34}]_{\Sigma3.00}{}^{W}(O_{0.94}F_{0.06})_{\Sigma1.00}$.

Lucchesiite is an oxy-species belonging to the calcic group of the tourmaline supergroup. The closest end-member composition of a valid tourmaline species is that of feruvite, to which lucchesiite is ideally related by the heterovalent coupled substitution $^{Z}Al^{3+} + {}^{O1}O^{2-} \leftrightarrow {}^{Z}Mg^{2+} + {}^{O1}(OH)^{1-}$. The new mineral was approved by the International Mineralogical Association Commission on New Minerals, Nomenclature and Classification (IMA 2015-043).

**KEYWORDS:** lucchesiite, new mineral species, crystal-structure refinement, electron microprobe, Mössbauer spectroscopy, infrared spectroscopy.

## Introduction

TOURMALINES are complex borosilicates that have been studied extensively in terms of their crystal structure and crystal chemistry (e.g. Foit, 1989; Grice and Ercit, 1993; Hawthorne, 1996, 2002; Hawthorne and Henry, 1999; Ertl *et al.*, 2002; Novák *et al.*, 2004; Bosi and Lucchesi, 2004, 2007; Bosi, 2010, 2013; Novák *et al.*, 2011; Henry and Dutrow, 2011; Filip *et al.*, 2012, Cempírek *et al.*, 2013). In accordance with Henry *et al.* (2011), the

*E-mail: ferdinando.bosi@uniroma1.it
https://doi.org/10.1180/minmag.2016.080.067

general formula of tourmaline is written as: $XY_3Z_6T_6O_{18}(BO_3)_3V_3W$, where X = $Na^+$, $K^+$, $Ca^{2+}$, □ (= vacancy); Y = $Al^{3+}$, $Fe^{3+}$, $Cr^{3+}$, $V^{3+}$, $Mg^{2+}$, $Fe^{2+}$, $Mn^{2+}$, $Li^+$; Z = $Al^{3+}$, $Fe^{3+}$, $Cr^{3+}$, $V^{3+}$, $Mg^{2+}$, $Fe^{2+}$; T = $Si^{4+}$, $Al^{3+}$, $B^{3+}$; B = $B^{3+}$; V = $(OH)^-$, $O^{2-}$; W = $(OH)^-$, $F^-$, $O^{2-}$. Note that the not italicized letters X, Y, Z and B represent groups of cations hosted in the $^{[9]}X$, $^{[6]}Y$, $^{[6]}Z$, $^{[4]}T$ and $^{[3]}B$ crystallographic sites (letters italicized). As for the letters V and W, they represent groups of anions accommodated at the [3]-coordinated O3 and O1 crystallographic sites, respectively. The dominance of specific ions at one or more sites of the structure gives rise to a range of distinct mineral species.

After publication of the recent tourmaline classification (Henry *et al.*, 2011), many new minerals of the tourmaline supergroup were approved by the Commission on New Minerals, Nomenclature and Classification (CNMNC) of the International Mineralogical Association (IMA): eleven of these minerals are oxy-species, two are hydroxy-species and four are fluor-species (Table 1).

A formal description of the new oxy-species lucchesiite is presented here. The mineral is named after Sergio Lucchesi (1958–2010), professor of mineralogy at Sapienza University of Rome (Italy), to honour his contribution to the study of tourmaline and spinel crystal chemistry. The new species and the new name have been approved by the IMA-CNMNC (proposal no. 2015-043). Two specimens of lucchesiite have been deposited: (1) the holotype specimen from Ratnapura, Sri Lanka, in the collections of the Museum of Mineralogy, Earth Sciences Department, Sapienza University of Rome, Italy, catalogue number 33198/1; (2) the cotype specimen from Mirošov, Czech Republic, in the Moravian Museum, Department of Mineralogy and Petrography, Zelný trh 6, Brno, Czech Republic, catalogue numbers A11137 (polished section with crystal used for the structure refinement) and A11138 (source sample). Note that the mineral assemblage, composition and crystal structure of the sample from the Czech Republic were described by Gadas *et al.* (2014), in which the sample was referred to as a 'feruvitic tourmaline'.

## Occurrence, appearance, physical and optical properties

The lucchesiite specimens examined here are from two distinct localities. With regard to the first, the crystal was acquired from a mineral trader who had

TABLE 1. New tourmalines approved by the IMA-CNMNC after Henry *et al.* (2011).

| Name | Formula | Reference |
|---|---|---|
| **Oxy-species** | | |
| Oxy-chromium-dravite | $NaCr_3(Cr_4Mg_2)(Si_6O_{18})(BO_3)_3(OH)_3O$ | Bosi *et al.* (2012*a*) |
| Oxy-dravite | $Na(Al_2Mg)(Al_5Mg)(Si_6O_{18})(BO_3)_3(OH)_3O$ | Bosi and Skogby (2013) |
| Oxy-schorl | $Na(Fe_2Al)Al_6(Si_6O_{18})(BO_3)_3(OH)_3O$ | Bačík *et al.* (2013) |
| Oxy-vanadium-dravite[a] | $NaV_3(V_4Mg_2)(Si_6O_{18})(BO_3)_3(OH)_3O$ | Bosi *et al.* (2013*a*) |
| Vanadio-oxy-dravite | $NaV_3(Al_4Mg_2)(Si_6O_{18})(BO_3)_3(OH)_3O$ | Bosi *et al.* (2014*a*) |
| Vanadio-oxy-chromium-dravite | $NaV_3(Cr_4Mg_2)(Si_6O_{18})(BO_3)_3(OH)_3O$ | Bosi *et al.* (2014*b*) |
| Chromo-alumino-povondraite | $NaCr_3(Al_4Mg_2)(Si_6O_{18})(BO_3)_3(OH)_3O$ | Reznitskii *et al.* (2014) |
| Darrellhenryite | $Na(LiAl_2)Al_6(Si_6O_{18})(BO_3)_3(OH)_3O$ | Novák *et al.* (2013*a*) |
| Maruyamaite | $K(Al_2Mg)(Al_5Mg)(Si_6O_{18})(BO_3)_3(OH)_3O$ | Lussier *et al.* (2016) |
| Bosiite | $NaFe_3(Al_4Mg_2)(Si_6O_{18})(BO_3)_3(OH)_3O$ | Ertl *et al.* (2016*a*) |
| Lucchesiite | $CaFe_3^{2+}Al_6(Si_6O_{18})(BO_3)_3(OH)_3O$ | This study |
| **Hydroxy-species** | | |
| Tsilaisite | $NaMn_3Al_6(Si_6O_{18})(BO_3)_3(OH)_3(OH)$ | Bosi *et al.* (2012*b*) |
| Adachiite | $CaFe_3Al_6(Si_5AlO_{18})(BO_3)_3(OH)_3(OH)$ | Nishio-Hamane *et al.* (2014) |
| **Fluor-species** | | |
| Fluor-dravite | $NaMg_3Al_6(Si_6O_{18})(BO_3)_3(OH)_3F$ | Clark *et al.* (2011) |
| Fluor-schorl | $NaFe_3Al_6(Si_6O_{18})(BO_3)_3(OH)_3F$ | Ertl *et al.* (2016*b*) |
| Fluor-elbaite | $Na(Li_{1.5}Al_{1.5})Al_6(Si_6O_{18})(BO_3)_3(OH)_3F$ | Bosi *et al.* (2013*b*) |
| Fluor-tsilaisite | $NaMn_3Al_6(Si_6O_{18})(BO_3)_3(OH)_3F$ | Bosi *et al.* (2015*a*) |

[a] Redefinition of the former mineral 'vanadium-dravite'.

labelled it 'fluor-feruvite from Sri Lanka, Ratnapura Gem Gravels'. The city of Ratnapura (6°35′N, 80°35′E) and the surrounding area is an important gemstone locality of Sri Lanka; the name of the city is from the Sanskrit words 'Pura' (= city) and 'Ratna' (= gemstone). There are numerous gem mines around the area which are mostly in alluvial deposits in gem-bearing river gravels ('illam') in ancient flood plains and streams now covered with farm land (Dahanayake, 1980; Munasinghe and Dissanayake, 1981; Dissanayake and Rupasinghe, 1993). The specimen is a part of a columnar crystal, the rupture being either of natural origin or deliberately made in order to split the sample into a larger number of specimens. Although the occurrence of gems in their rock-matrix is rare, they are most probably associated with pegmatites. Alluvial gem deposits do not necessarily occur close to the area where they originate, though most concentrations of alluvial gem beds are close to their source area (Herat, 1984; Mendis *et al.*, 1993). Lucchesiite was also found in an anatectic pegmatite from Mirošov near Strážek, western Moravia, Czech Republic (49°27′49.38″N, 16°9′54.34″E). An irregularly-shaped pegmatite dyke, up to 20 cm thick, cuts calc-silicate rock and contains the following minerals: major plagioclase ($An_{30–42}$), quartz and K-feldspar, minor amphibole and tourmaline in three textural-paragenetic forms; interstitial Ca-rich schorl–dravite to Na-Mg-rich feruvite in an outer granitic unit, graphic intergrowths of Ca-rich schorl to Na-rich lucchesiite with quartz in the central parts of the pegmatite, and volumetrically subordinate Ca-rich dravite replacing both previous forms of tourmaline occasionally (Gadas *et al.*, 2014). The anatectic pegmatite evolved from migmatitic leucosome of the surrounding amphibole-biotite gneiss to amphibolite complex and was contaminated from the host calc-silicate rock as manifested by the Ca-rich mineral assemblage.

The lucchesiite crystal from Sri Lanka shows anhedral habitus (up to ~5 mm), as a broken part of a columnar crystal, whereas that from the Czech Republic forms graphic intergrowths with quartz in large aggregates up to 5 cm (Fig. 1). Lucchesiite is black with a vitreous lustre. It has a grey streak and shows no fluorescence. Lucchesiite has a Mohs hardness of ~7, and is brittle with a conchoidal fracture inferred from the Sri Lanka crystal. The calculated density is 3.209 g/cm$^3$ (Sri Lanka) and 3.243 g/cm$^3$ (Czech Republic). In thin section, lucchesiite is transparent; in transmitted light, the investigated lucchesiite thin-section samples are pleochroic with O = very dark brown and E = light brown (Sri Lanka) and O = opaque and E = dark brown (Czech Republic). Lucchesiite is uniaxial (–) with refractive indices as follows: for the Sri Lanka sample, $\omega = 1.670(5)$ and $\varepsilon = 1.655(5)$ measured by the immersion method using white light from a tungsten source; for the Czech Republic sample, $\omega$ could not be measured as a consequence of opacity in the optical O-direction and $\varepsilon = 1.656(6)$ measured with gel filtered Na light ($\lambda = 589.9$ nm). The mean index of refraction, density, and composition lead to an excellent compatibility index for the Sri Lanka sample ($1 - Kp/Kc = 0.03$) (Mandarino, 1981).

FIG. 1. Photo of lucchesiite from Mirošov, Czech Republic; the field of view is 12 cm, and the height of the graphic intergrowths of lucchesiite and quartz is 5 cm.

## Experimental methods and results

### *Single-crystal structure refinement*

A representative black crystal of lucchesiite from Sri Lanka was selected for X-ray diffraction measurements on a Bruker KAPPA APEX-II single-crystal diffractometer (Sapienza University of Rome, Earth Sciences Department), equipped with a CCD area detector (6.2 cm × 6.2 cm active detection area, 512 × 512 pixels) and a graphite-crystal monochromator, using Mo$K\alpha$ radiation from a fine-focus sealed X-ray tube. The sample-to-detector distance was 4 cm. A total of 3681 exposures (step = 0.2°, time/step = 20 s) covering a full reciprocal sphere with a redundancy of ~12 was collected. Final unit-cell parameters were refined using the Bruker AXS *SAINT* program on reflections with $I > 10\sigma(I)$ in the range $5° < 2\theta < 81°$. The intensity data were processed and corrected for

Lorentz, polarization and background effects using the *APEX2* software program of Bruker AXS. The data were corrected for absorption using a multi-scan method (*SADABS*). The absorption correction led to a significant improvement in $R_{int}$. No violation of *R*3*m* symmetry was detected.

Structure refinement was carried out using the *SHELXL-2013* program (Sheldrick, 2013). Starting coordinates were taken from Bosi *et al.* (2015*b*). Variable parameters were: scale factor, extinction coefficient, atom coordinates, site-scattering values (for *X*, *Y* and *Z* sites) and atomic-displacement factors. Neutral scattering factors were used for all the atoms. In detail, the *X* site was modelled using the Ca scattering factor. The occupancy of the *Y* site was obtained considering the presence of Fe *vs.* Mg, and the *Z* site by Al. The *T*, *B* and anion sites were modelled, respectively, with Si, B and O scattering factors and with a fixed occupancy of 1, because refinement with unconstrained occupancies showed no significant deviations from this value. There were no correlations greater than 0.7 between the parameters at the end of the refinement. Table 2 lists crystal data, data-collection information and refinement details; Table 3 gives the fractional atom coordinates, equivalent isotropic-displacement parameters; Table 4 contains anisotropic-displacement parameters; Table 5 shows selected bond lengths. A crystallographic information file has been deposited with the Principal Editor of *Mineralogical Magazine* and is available from http://www.minersoc.org/pages/e_journals/dep_mat_mm.html.

Selected crystallographic data for lucchesiite from the Czech Republic (Gadas *et al.*, 2014) are also reported in Tables 2 and 5 for comparison.

TABLE 2. Single-crystal X-ray diffraction data for lucchesiite

| Sample | Sri Lanka | Czech Republic[a] |
|---|---|---|
| Crystal size (mm) | 0.13 × 0.20 × 0.21 | 0.07 × 0.07 × 0.05 |
| *a* (Å) | 16.0018(7) | 16.0047(4) |
| *c* (Å) | 7.2149(3) | 7.2120(2) |
| *V* (Å$^3$) | 1599.92(15) | 1599.86(7) |
| Range for data collection, 2θ (°) | 5–81 | 6–73 |
| Reciprocal space range *hkl* | $-28 \le h \le 25$<br>$-17 \le k \le 25$<br>$-12 \le l \le 12$ | $-26 \le h \le 26$<br>$-26 \le k \le 26$<br>$-11 \le l \le 11$ |
| Observed reflections | 14,040 | 18,675 |
| Unique reflections, $R_{int}$ (%) | 2244, 1.98 | 1725, 4.1 |
| Redundancy | 12 | 8 |
| Absorption correction method | *SADABS* | *SADABS* |
| Refinement method | Last-squares on $F^2$ | Last-squares on $F^2$ |
| Structural refinement program | SHELXL-2013 | SHELXL-97 |
| Extinction coefficient | 0.0221(6) | 0.00130(13) |
| Flack parameter | 0.068(12) | 0.007(9) |
| *wR*2 (%) | 3.68 | 3.53 |
| *R*1 (%) all data | 1.51 | 1.57 |
| *R*1 (%) for $I > 2\sigma(I)$ | 1.49 | 1.53 |
| Goof | 1.064 | 1.023 |
| Peaks = peak and hole ($\pm e^-$/Å$^3$) | –0.54 and 0.45 | –0.49 and 0.53 |

Space group *R*3*m*; *Z* = 3. Radiation, Mo*K*α = 0.71073 Å. Data collection temperature = 293 K. $R_{int}$ = merging residual value; *R*1 = discrepancy index, calculated from *F*-data; *wR*2 = weighted discrepancy index, calculated from $F^2$-data; Goof = goodness of fit; Peaks = maximum and minimum residual electron density.
[a]From Gadas *et al.* (2014).

## Powder X-ray diffraction

The powder X-ray diffraction pattern for lucchesiite from Sri Lanka was collected using a Panalytical X'pert powder diffractometer equipped with an X'celerator silicon-strip detector. The range 5–80° (2θ) was scanned with a step-size of 0.017° using a sample spinner with the sample mounted on a background-free holder. The diffraction data (for Cu*K*α = 1.54059), Å corrected using Si as an internal standard, are listed in Table 6. The program *UnitCell* (Holland and Redfern, 1997) was used to refine unit-cell parameters in the trigonal system: *a* = 16.006(3) Å, *c* = 7.2136(2) Å and *V* = 1599.39(6) Å$^3$.

The powder X-ray diffraction data for the Czech Republic sample led to the unit-cell parameters *a* = 16.0159(2), *c* = 7.2363(1) Å and *V* = 1607.48(5) Å$^3$ (Gadas *et al.* 2014). The indexed powder X-ray diffraction pattern, not shown in Gadas *et al.* (2014) is listed in Table 6.

## Microprobe analysis

Electron microprobe analysis for the sample from Sri Lanka was undertaken using a wavelength-dispersive spectrometer (WDS mode) with a Cameca SX50 instrument at the 'Istituto di

TABLE 3. Fractional atom coordinates and refined site occupancy for lucchesiite (Sri Lanka).

| Site | *x* | *y* | *z* | Site occupancy |
|---|---|---|---|---|
| *X* | 0 | 0 | 0.21896(10) | $Ca_{0.887(5)}$ |
| *Y* | 0.12351(2) | 0.06175(2) | 0.63485(5) | $Fe_{0.574(4)}Mg_{0.426(4)}$ |
| *Z* | 0.29841(2) | 0.26170(2) | 0.61159(6) | $Al_{1.031(3)}$ |
| *B* | 0.11016(5) | 0.22032(11) | 0.4515(2) | $B_{1.00}$ |
| *T* | 0.19183(2) | 0.19016(2) | 0 | $Si_{1.00}$ |
| O1 (≡W) | 0 | 0 | 0.7845(3) | $O_{1.00}$ |
| O2 | 0.06064(4) | 0.12128(8) | 0.47420(18) | $O_{1.00}$ |
| O3 (≡V) | 0.26809(9) | 0.13405(5) | 0.51165(16) | $O_{1.00}$ |
| O4 | 0.09201(4) | 0.18402(9) | 0.07168(15) | $O_{1.00}$ |
| O5 | 0.18195(9) | 0.09098(5) | 0.09124(15) | $O_{1.00}$ |
| O6 | 0.19619(6) | 0.18734(6) | 0.77810(11) | $O_{1.00}$ |
| O7 | 0.28488(5) | 0.28426(5) | 0.08032(11) | $O_{1.00}$ |
| O8 | 0.20923(6) | 0.26987(6) | 0.44146(12) | $O_{1.00}$ |
| H3 | 0.263(2) | 0.1314(10) | 0.388(4) | $H_{1.00}$ |

TABLE 4. Displacement parameters (Å$^2$) for lucchesiite (Sri Lanka).

| Site | $U^{11}$ | $U^{22}$ | $U^{33}$ | $U^{23}$ | $U^{13}$ | $U^{12}$ | $U_{eq}/U_{iso}$* |
|---|---|---|---|---|---|---|---|
| *X* | 0.0149(2) | 0.0149(2) | 0.0183(3) | 0 | 0 | 0.00745(11) | 0.01605(18) |
| *Y* | 0.00925(14) | 0.00593(11) | 0.01230(13) | –0.00253(4) | –0.00506(8) | 0.00463(7) | 0.00879(9) |
| *Z* | 0.00530(13) | 0.00566(13) | 0.00592(11) | 0.00056(9) | –0.00002(8) | 0.00258(10) | 0.00570(8) |
| *B* | 0.0058(4) | 0.0059(5) | 0.0085(5) | 0.0004(4) | 0.0002(2) | 0.0030(3) | 0.0067(2) |
| *T* | 0.00471(12) | 0.00452(11) | 0.00636(11) | –0.00050(8) | –0.00035(8) | 0.00217(8) | 0.00526(7) |
| O1 | 0.0177(6) | 0.0177(6) | 0.0178(8) | 0 | 0 | 0.0089(3) | 0.0177(4) |
| O2 | 0.0116(3) | 0.0059(4) | 0.0128(4) | 0.0015(3) | 0.00077(15) | 0.0029(2) | 0.0107(2) |
| O3 | 0.0174(5) | 0.0130(3) | 0.0067(3) | 0.00057(17) | 0.0011(3) | 0.0087(3) | 0.01188(19) |
| O4 | 0.0077(3) | 0.0153(5) | 0.0103(4) | –0.0011(3) | –0.00056(17) | 0.0076(2) | 0.01025(18) |
| O5 | 0.0151(5) | 0.0078(3) | 0.0099(4) | 0.00074(17) | 0.0015(3) | 0.0076(2) | 0.01012(18) |
| O6 | 0.0104(3) | 0.0093(3) | 0.0066(2) | –0.0010(2) | –0.0004(2) | 0.0052(2) | 0.00864(13) |
| O7 | 0.0079(3) | 0.0065(3) | 0.0096(3) | –0.0010(2) | –0.0020(2) | 0.0019(2) | 0.00878(13) |
| O8 | 0.0050(3) | 0.0092(3) | 0.0153(3) | 0.0021(2) | 0.0006(2) | 0.0032(2) | 0.01003(14) |
| H3 | | | | | | | 0.014* |

Equivalent ($U_{eq}$) and isotropic ($U_{iso}$) displacement parameters; H-atom was constrained to have a $U_{iso}$ 1.2 times the $U_{eq}$ value of the O3 oxygen.

Geologia Ambientale e Geoingegneria (Rome, Italy), CNR', operating at an accelerating potential of 15 kV a sample current of 15 nA and 10 μm beam diameter. Minerals and synthetic compounds were used as standards: wollastonite (Si, Ca), magnetite (Fe), rutile (Ti), corundum (Al), vanadinite (V), fluorphlogopite (F), periclase (Mg), jadeite (Na), orthoclase (K), sphalerite (Zn), rhodonite (Mn), metallic Cr and Cu. The 'PAP' routine was applied (Pouchou and Pichoir, 1991). The results (Table 7) represent mean values of 10 spot analyses. In accord with the very low concentration of Li in Mg-rich tourmaline samples (e.g. Henry *et al.*, 2011) and the results from Gadas *et al.* (2014) on lucchesiite from the Czech Republic (Li 16–17 ppm), the $Li_2O$ content was assumed to be insignificant in the lucchesiite from Sri Lanka. Chromium and Cu were below their respective detection limits (0.02 wt.%) in the sample studied.

For lucchesiite from the Czech Republic, the FeO, $Fe_2O_3$ and $H_2O$ values listed in the original

TABLE 5. Selected bond lengths (Å) in lucchesiite.

| Sample | Sri Lanka | Czech Republic[a] |
|---|---|---|
| *X*–O2 (× 3) | 2.4932(13) | 2.5242(15) |
| *X*–O5 (× 3) | 2.6845(12) | 2.6920(11) |
| *X*–O4 (× 3) | 2.7626(12) | 2.7640(12) |
| <*X*–O> | 2.647 | 2.660 |
| *Y*–O1 | 2.0235(14) | 1.9993(16) |
| *Y*–O6 (× 2) | 2.0303(8) | 2.0383(8) |
| *Y*–O2(× 2) | 2.0545(8) | 2.0468(9) |
| *Y*–O3 | 2.1919(13) | 2.2180(12) |
| <*Y*–O> | 2.064 | 2.095 |
| *Z*–O6 | 1.8942(9) | 1.8909(9) |
| *Z*–O8 | 1.9024(8) | 1.9017(8) |
| *Z*–O7 | 1.9050(8) | 1.9040(8) |
| *Z*–O8' | 1.9356(9) | 1.9344(8) |
| *Z*–O7' | 1.9731(8) | 1.9756(8) |
| *Z*–O3 | 1.9842(6) | 1.9826(6) |
| <*Z*–O> | 1.932 | 1.932 |
| *B*–O2 | 1.3823(19) | 1.3788(18) |
| *B*–O8 (× 2) | 1.3748(11) | 1.3765(10) |
| <*B*–O> | 1.377 | 1.377 |
| *T*–O6 | 1.6041(8) | 1.6047(10) |
| *T*–O7 | 1.6057(7) | 1.6063(7) |
| *T*–O4 | 1.6344(4) | 1.6317(5) |
| *T*–O5 | 1.6512(5) | 1.6494(6) |
| <*T*–O> | 1.624 | 1.623 |

[a]From Gadas *et al.* (2014).

publication (analysis TU2# in table 2 of Gadas *et al.*, 2014) are incorrect. Correct chemical data are provided here (Table 7) on the basis of the final formula optimized from the single-crystal diffraction data (Gadas *et al.*, 2014).

### *Mössbauer spectroscopy*

In order to determine the $Fe^{3+}/\Sigma Fe$ ratio for lucchesiite from Sri Lanka, a crystal fragment was ground under acetone and analysed using $^{57}Fe$ Mössbauer spectroscopy with a conventional spectrometer system operated in constant acceleration mode. Data were collected over 1024 channels and were folded and calibrated against the spectrum of an α-Fe foil. The lucchesiite spectrum (Fig. 2) was fitted using the software *MossA* (Prescher *et al.*, 2012) with three doublets assigned to $Fe^{2+}$ and one doublet assigned to $Fe^{3+}$, resulting in an $Fe^{3+}/\Sigma Fe$ ratio of 0.15. The obtained hyperfine parameters (Table 8) are consistent with $Fe^{2+}$ at the *Y* site and $Fe^{3+}$ at the *Z* site (cf. Andreozzi *et al.*, 2008). However, a unique Fe site-distribution cannot be achieved due to the limited resolution of the absorption doublets.

The Mössbauer spectrum for the Czech Republic sample, showed in Gadas *et al.* (2014), resulted in an $Fe^{3+}/\Sigma Fe$ ratio of 0.45, that includes half of an intervalence charge transfer component. The detailed spectral parameters and their assignment are listed in Gadas *et al.* (2014).

### *Single-crystal infrared spectroscopy*

To obtain information on the hydrogen speciation in the holotype specimen from Sri Lanka, Fourier transform infrared (FTIR) absorption spectra in the range of 2000–5000 $cm^{-1}$ were measured on an oriented 39 μm thick single-crystal section. A Bruker Vertex spectrometer equipped with a halogen lamp source, a $CaF_2$ beamsplitter, a KRS-5 wiregrid polarizer and an InSb detector were used to collect spectra at a resolution of 2 $cm^{-1}$. Spectra recorded in polarized mode perpendicular and parallel to the crystallographic **c** axis show an intense band around 3570 $cm^{-1}$ and some very weak bands at 3710–3760 $cm^{-1}$, all strongly polarized in the **c**-axis direction (Fig. 3). As observed typically for tourmaline spectra in the (OH) range, the main band is off-scale for the **E**//**c** direction due to excessive absorption (e.g. Gebert and Zemann, 1965).

It is worth noting the lack of significant bands above *c.* 3650 $cm^{-1}$, which is the region where bands due to (OH) are expected at the W position (e.g. Gonzalez-Carreño *et al.*, 1988; Skogby *et al.*, 2012; Bosi *et al.*, 2015*c*). This observation is consistent with the very low concentrations of (OH) at the W position obtained from the other methods.

### *Determination of number of atoms per formula unit (apfu)*

In agreement with the structure-refinement results, the boron content was assumed to be stoichiometric ($B^{3+} = 3.00$ apfu). Both the site-scattering results and the bond lengths of *B* and *T* are consistent with the *B* site fully occupied by boron and no amount of $B^{3+}$ at the *T* site (e.g. Hawthorne, 1996; Bosi and Lucchesi, 2007). For the Sri Lanka sample, the ratio $Fe^{3+}/\Sigma Fe = 0.15$ was determined by Mössbauer spectroscopy. For the sample from the Czech Republic, the ratio $Fe^{3+}/\Sigma Fe = 0.54$ was optimized without constraints to Mössbauer spectroscopy data due to its inhomogeneous Fe contents. Note that this value is close to that determined by Mössbauer

TABLE 6. Powder X-ray diffraction patterns for lucchesiite.

| Sample | | | Sri Lanka | | | Czech Republic | | |
|---|---|---|---|---|---|---|---|---|
| *h* | *k* | *l* | *I* | $d_{meas}$ | $d_{cal}$ | *I* | $d_{meas}$ | $d_{cal}$ |
| 1 | 1 | 0 | 2 | 7.988 | 8.000 | 3 | 8.024 | 8.012 |
| **1** | **0** | **1** | **24** | **6.390** | **6.399** | **53** | **6.424** | **6.419** |
| 0 | 2 | 1 | 15 | 4.992 | 4.997 | 20 | 5.011 | 5.010 |
| 0 | 3 | 0 | 13 | 4.615 | 4.619 | 15 | 4.627 | 4.626 |
| **2** | **1** | **1** | **42** | **4.236** | **4.238** | **41** | **4.249** | **4.248** |
| 2 | 2 | 0 | 36 | 3.999 | 4.000 | 29 | 4.007 | 4.006 |
| **0** | **1** | **2** | **72** | **3.490** | **3.491** | **100** | **3.503** | **3.503** |
| 1 | 3 | 1 | 6 | 3.391 | 3.392 | 5 | 3.399 | 3.399 |
| 2 | 0 | 2 | 2 | 3.199 | 3.199 | 3 | 3.210 | 3.210 |
| 4 | 0 | 1 | – | | | 1 | 3.128 | 3.129 |
| 1 | 4 | 0 | 10 | 3.024 | 3.024 | 8 | 3.028 | 3.028 |
| **1** | **2** | **2** | **99** | **2.970** | **2.971** | **100** | **2.979** | **2.979** |
| 3 | 2 | 1 | 11 | 2.909 | 2.909 | 7 | 2.914 | 2.914 |
| 3 | 1 | 2 | 8 | 2.630 | 2.630 | 6 | 2.637 | 2.637 |
| **0** | **5** | **1** | **100** | **2.587** | **2.587** | **84** | **2.591** | **2.592** |
| 0 | 4 | 2 | 5 | 2.498 | 2.499 | 5 | 2.505 | 2.505 |
| 2 | 4 | 1 | 5 | 2.461 | 2.462 | 4 | 2.466 | 2.466 |
| 0 | 0 | 3 | 18 | 2.404 | 2.405 | 22 | 2.413 | 2.413 |
| 2 | 3 | 2 | 19 | 2.385 | 2.385 | 15 | 2.391 | 2.391 |
| 5 | 1 | 1 | 14 | 2.353 | 2.353 | 9 | 2.357 | 2.357 |
| 0 | 6 | 0 | 3 | 2.309 | 2.310 | 3 | 2.312 | 2.313 |
| 5 | 2 | 0 | 2 | 2.219 | 2.219 | 1 | 2.222 | 2.222 |
| 5 | 0 | 2 | 17 | 2.198 | 2.198 | 12 | 2.203 | 2.203 |
| 4 | 3 | 1 | 16 | 2.172 | 2.172 | 10 | 2.176 | 2.176 |
| 3 | 0 | 3 | 26 | 2.133 | 2.133 | 22 | 2.139 | 2.140 |
| 4 | 2 | 2 | 8 | 2.119 | 2.119 | 5 | 2.124 | 2.124 |
| 2 | 2 | 3 | 30 | 2.061 | 2.061 | 19 | 2.067 | 2.067 |
| **1** | **5** | **2** | **69** | **2.049** | **2.048** | **49** | **2.053** | **2.053** |
| 1 | 6 | 1 | 12 | 2.028 | 2.028 | 8 | 2.031 | 2.031 |
| 4 | 4 | 0 | 5 | 2.000 | 2.000 | 3 | 2.003 | 2.003 |
| **3** | **4** | **2** | **43** | **1.926** | **1.926** | **17** | **1.930** | **1.930** |
| 3 | 5 | 1 | – | | | 2 | 1.912 | 1.912 |
| 1 | 4 | 3 | 14 | 1.882 | 1.882 | 11 | 1.887 | 1.887 |
| 6 | 2 | 1 | 9 | 1.857 | 1.857 | 6 | 1.860 | 1.860 |
| 6 | 1 | 2 | 2 | 1.823 | 1.823 | 3 | 1.818 | 1.827 |
| 3 | 3 | 3 | 9 | 1.786 | 1.786 | 4 | 1.791 | 1.791 |
| 0 | 2 | 4 | 8 | 1.745 | 1.745 | 6 | 1.752 | 1.751 |
| 0 | 7 | 2 | 3 | 1.735 | 1.735 | 2 | 1.739 | 1.739 |
| 2 | 1 | 4 | 1 | 1.705 | 1.705 | 1 | 1.710 | 1.711 |
| 2 | 6 | 2 | 5 | 1.696 | 1.696 | 2 | 1.699 | 1.699 |
| 0 | 6 | 3 | 38 | 1.666 | 1.666 | 22 | 1.670 | 1.670 |
| 2 | 7 | 1 | 18 | 1.648 | 1.648 | 8 | 1.651 | 1.651 |
| 1 | 3 | 4 | – | | | 1 | 1.636 | 1.638 |
| 5 | 5 | 0 | 32 | 1.600 | 1.600 | 11 | 1.603 | 1.602 |
| 4 | 5 | 2 | 6 | 1.592 | 1.592 | – | | |
| 8 | 1 | 1 | 2 | 1.582 | 1.582 | 2 | 1.585 | 1.585 |
| 3 | 2 | 4 | 4 | 1.569 | 1.569 | 3 | 1.573 | 1.574 |
| 4 | 6 | 1 | 4 | 1.552 | 1.552 | 2 | 1.555 | 1.555 |
| 0 | 9 | 0 | 5 | 1.540 | 1.540 | 3 | 1.542 | 1.542 |
| 7 | 2 | 2 | 7 | 1.533 | 1.533 | 4 | 1.535 | 1.535 |
| 7 | 3 | 1 | 2 | 1.524 | 1.524 | – | | |

*(continued)*

TABLE 6. (*contd.*)

| Sample | | | Sri Lanka | | | Czech Republic | | |
|---|---|---|---|---|---|---|---|---|
| *h* | *k* | *l* | *I* | $d_{meas}$ | $d_{cal}$ | *I* | $d_{meas}$ | $d_{cal}$ |
| **0** | **5** | **4** | **42** | **1.512** | **1.512** | **16** | **1.516** | **1.516** |
| 8 | 2 | 0 | – | | | 3 | 1.515 | 1.514 |
| 2 | 4 | 4 | 9 | 1.485 | 1.485 | 6 | 1.490 | 1.490 |
| 1 | 8 | 2 | 2 | 1.479 | 1.479 | – | | |
| 5 | 1 | 4 | 38 | 1.460 | 1.460 | 16 | 1.464 | 1.465 |
| 0 | 1 | 5 | 18 | 1.435 | 1.435 | 9 | 1.440 | 1.440 |
| 6 | 5 | 1 | 10 | 1.424 | 1.424 | 6 | 1.426 | 1.426 |
| 4 | 3 | 4 | 24 | 1.414 | 1.414 | 8 | 1.418 | 1.418 |
| 3 | 8 | 1 | 2 | 1.381 | 1.381 | 1 | 1.384 | 1.383 |
| 10 | 0 | 1 | 15 | 1.361 | 1.361 | 5 | 1.363 | 1.363 |
| 5 | 6 | 2 | 6 | 1.348 | 1.347 | 3 | 1.350 | 1.350 |
| 6 | 6 | 0 | 16 | 1.333 | 1.333 | 8 | 1.336 | 1.335 |
| 6 | 2 | 4 | 17 | 1.315 | 1.315 | 6 | 1.318 | 1.319 |
| 5 | 7 | 1 | 2 | 1.305 | 1.305 | – | | |
| 9 | 0 | 3 | 1 | 1.297 | 1.297 | – | | |
| 0 | 10 | 2 | 3 | 1.294 | 1.294 | 2 | 1.296 | 1.296 |
| 8 | 4 | 1 | 2 | 1.288 | 1.288 | – | | |
| 5 | 0 | 5 | 34 | 1.280 | 1.280 | 12 | 1.284 | 1.284 |
| 5 | 4 | 4 | 5 | 1.265 | 1.265 | 2 | 1.268 | 1.268 |
| 0 | 11 | 1 | 7 | 1.241 | 1.241 | 1 | 1.243 | 1.243 |
| 7 | 4 | 3 | 3 | 1.234 | 1.233 | 1 | 1.237 | 1.236 |
| 4 | 8 | 2 | 5 | 1.231 | 1.231 | 1 | 1.233 | 1.233 |
| 3 | 4 | 5 | 4 | 1.219 | 1.219 | 3 | 1.223 | 1.223 |
| 0 | 0 | 6 | 5 | 1.202 | 1.202 | 3 | 1.207 | 1.207 |

$I$ = measured intensity (%), $d_{meas}$ = measured interplanar spacing (Å);
$d_{calc}$ = calculated interplanar spacing (Å); *hkl* = reflection indices.
Estimated errors in measured *d*-values range from 0.01 Å for large *d*-values to 0.001 Å for small *d*-values.
The eight reflections with the highest intensity are in bold.

spectroscopy ($Fe^{3+}/\Sigma Fe = 0.45$; Gadas *et al.*, 2014). The formulae and (OH) contents were then calculated by charge balance under the assumption of $T + Y + Z = 15$ apfu and 31 anions. The number of apfu were calculated on this assumption (Table 7). The excellent agreement between the number of electrons per formula unit (epfu) derived from EMPA and SREF (257.8 epfu *vs.* 257.3 epfu and 263.1 epfu *vs.* SREF 262.8 epfu, for the Sri Lanka and Czech Republic specimens, respectively) supports the stoichiometric assumptions.

### *Site populations*

With regard to the Sri Lanka sample, the site populations at the *X*, *B*, *T*, O3 (≡ V) and O1 (≡ W) sites follow the standard site preference suggested for tourmaline (e.g. Henry *et al.*, 2011) and are coherent with the information from FTIR absorption spectra (Fig. 3), whereas the site populations at the octahedrally coordinated *Y* and *Z* sites were optimized according to the procedure of Bosi and Lucchesi (2007) and Wright *et al.* (2000), and by fixing the minor elements $Ti^{4+}$, $V^{3+}$, $Mn^{2+}$ and Zn at *Y* and $Fe^{3+}$ at *Z*.

The resulting empirical formula of the Sri Lanka sample is:

$$^{X}(Ca_{0.69}Na_{0.30}K_{0.02})_{\Sigma 1.01}$$
$$^{Y}\left(Fe^{2+}_{1.44}Mg_{0.72}Al_{0.48}Ti^{4+}_{0.33}V^{3+}_{0.02}Mn_{0.01}Zn_{0.01}\right)_{\Sigma 3.00}$$
$$^{Z}\left(Al_{4.74}Mg_{1.01}Fe^{3+}_{0.25}\right)_{\Sigma 6.00}\left[^{T}(Si_{5.85}Al_{0.15})_{\Sigma 6.00}O_{18}\right]$$
$$(BO_3)_3{}^{V}(OH)_3{}^{W}\left[O^{2-}_{0.69}F_{0.24}(OH)_{0.07}\right]_{\Sigma 1.00}$$

After the corrections mentioned above, the

TABLE 7. Composition of lucchesiite.

| Sample | Sri Lanka (10 spots) | | Czech Republic[a] (5 spots) | |
|---|---|---|---|---|
| | Average | Range | Average | Range |
| $SiO_2$ wt.% | 34.03(19) | 33.62–34.24 | 33.46(25) | 33.13–33.75 |
| $TiO_2$ | 2.53(5) | 2.49–2.61 | 0.64(1) | 0.62–0.65 |
| $B_2O_3$ | 10.11[b] | – | 9.89[b] | – |
| $Al_2O_3$ | 26.48(17) | 26.17–26.82 | 27.00(17) | 26.68–27.19 |
| $V_2O_3$ | 0.12(2) | 0.11–0.16 | b.d.l. | – |
| $FeO_{tot}$ | 11.77(13) | 11.54–11.93 | 16.82(14) | 16.64–17.02 |
| MgO | 6.73(9) | 6.67–6.95 | 3.59(5) | 3.51–3.64 |
| MnO | 0.05(3) | 0.00–0.09 | 0.20(1) | 0.18–0.22 |
| ZnO | 0.10(7) | 0.00–0.21 | 0.04(3) | 0.00–0.08 |
| CaO | 3.74(7) | 3.61–3.82 | 2.62(4) | 2.59–2.70 |
| $Na_2O$ | 0.89(2) | 0.92–0.84 | 1.32(3) | 1.28–1.37 |
| $K_2O$ | 0.09(1) | 0.07–0.11 | 0.06(1) | 0.04–0.07 |
| F | 0.44(8) | 0.34–0.57 | 0.10(1) | 0.09–0.12 |
| $H_2O$ | 2.67[b] | – | 2.27(5)[b] | – |
| –O=F | –0.19 | | –0.04 | |
| $Fe_2O_3$ | 1.97[c] | | 10.05[d] | |
| FeO | 10.00[c] | | 7.77[d] | |
| Total | 99.76 | | 98.96 | |
| | Atoms normalized to 31 anions | | | |
| Si (apfu) | 5.85 | | 5.88 | |
| $Ti^{4+}$ | 0.33 | | 0.08 | |
| B | 3.00 | | 3.00 | |
| Al | 5.37 | | 5.59 | |
| $V^{3+}$ | 0.02 | | – | |
| $Fe^{3+}$ | 0.25 | | 1.33 | |
| $Fe^{2+}$ | 1.44 | | 0.95 | |
| $Mn^{2+}$ | 0.01 | | 0.03 | |
| Zn | 0.01 | | 0.01 | |
| Ca | 0.67 | | 0.49 | |
| Na | 0.30 | | 0.45 | |
| K | 0.02 | | 0.01 | |
| F | 0.24 | | 0.06 | |
| OH | 3.07 | | 2.66 | |

[a]The FeO, $Fe_2O_3$ and $H_2O$ values listed in the original publication (analysis TU2#, table 2 of Gadas *et al.*, 2014) are incorrect; the correct values are provide here.
[b]Calculated by stoichiometry.
[c]Determined by Mössbauer spectroscopy.
[d]From formula optimization combined with Mössbauer spectroscopy.
Errors for oxides are standard deviations (in brackets) of several spot analyses; b.d.l. = below detection limits, apfu = atoms per formula unit.

empirical formula of the Czech Republic sample is:

$$^{X}(Ca_{0.49}Na_{0.45}\square_{0.05}K_{0.01})_{\Sigma 1.00}$$
$$^{Y}\left(Fe^{2+}_{1.14}Fe^{3+}_{0.95}Mg_{0.42}Al_{0.37}Mn_{0.03}Ti^{4+}_{0.08}Zn_{0.01}\right)_{\Sigma 3.00}$$
$$^{Z}\left(Al_{5.11}Mg_{0.52}Fe^{3+}_{0.38}\right)_{\Sigma 6.00}\left[^{T}(Si_{5.88}Al_{0.12})_{\Sigma 6.00}O_{18}\right]$$
$$(BO_3)_3{}^{V}\left[(OH)_{2.66}O_{0.34}\right]_{\Sigma 3.00}{}^{W}(O_{0.94}F_{0.06})_{\Sigma 1.00}.$$

## End-member formula, name, relation to other species and geological environment of lucchesiite

The empirical formula of the present samples are consistent with a tourmaline belonging to the calcic group (Henry *et al.*, 2011): Ca-dominant at the X position of the tourmaline general formula and oxygen-dominant at W with $O^{2-} > (F + OH)^{1-}$. The

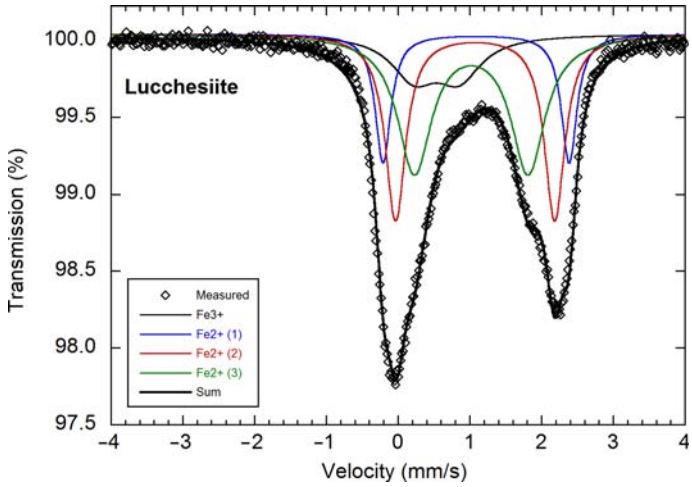


FIG. 2. Room-temperature Mössbauer spectrum for lucchesiite from Sri Lanka.

*Z* site is dominated by Al and the *Y* site is dominated by $Fe^{2+}$. Consequently, the end-member formula can be represented as $CaFe^{2+}_3Al_6(Si_6O_{18})(BO_3)_3(OH)_3O$. As no tourmalines have yet been proposed with this end-member composition, the tourmalines studied can be classified as a new species with the name lucchesiite.

The closest end-member composition of a valid tourmaline species is that of feruvite, $CaFe^{2+}_3(Al_5Mg)(Si_6O_{18})(BO_3)_3(OH)_3(OH)$, to which lucchesiite is related by the heterovalent substitution $^{Z}Al^{3+} + {}^{O1}O^{2-} \leftrightarrow {}^{Z}Mg^{2+} + {}^{O1}(OH)^{1-}$. As the lucchesiite composition is generated through a heterovalent coupled substitution involving two sites (*Z* and O1) of an existing end-member (feruvite), a new root name is warranted rather than placing a modifying prefix to an existing root name, in accordance with the tourmaline nomenclature in force (Henry *et al.*, 2011).

TABLE 8. Mössbauer parameters for lucchesiite from Sri Lanka obtained at room-temperature.

| δ | $\Delta E_Q$ | Γ | % Area | Assignment |
|---|---|---|---|---|
| 1.08 | 2.59 | 0.26 | 16.3 | $^{VI}Fe^{2+}$ |
| 1.07 | 2.22 | 0.34 | 30.8 | $^{VI}Fe^{2+}$ |
| 1.02 | 1.58 | 0.57 | 37.8 | $^{VI}Fe^{2+}$ |
| 0.53 | 0.62 | 0.76 | 15.0 | $^{VI}Fe^{3+}$ |

$\delta$ = centroid shift (mm/s), $\Delta E_Q$ = quadrupole splitting (mm/s), Γ = full width (mm/s). Estimated errors for these parameters are ±0.02 mm/s.

Comparative data for lucchesiite and feruvite (Grice and Robinson, 1989) are given in Table 9. On the basis of available information, lucchesiite and feruvite may be distinguished by their unit-cell parameters and their refractive indices, which are both correlated inversely with the Al contents due to the relative small size of $Al^{3+}$ (e.g. Bosi *et al.*, 2010) and its relative small atomic number (=13). Ideally, lucchesiite has larger Al contents than feruvite, and hence smaller unit-cell parameters ($a$ = 16.00 *vs.* 16.01 Å, $c$ = 7.21 *vs.* 7.25 Å) and refractive indices (ω = 1.67 *vs.* 1.69 and ε = 1.66 *vs.* 1.67). However, due to the complex crystal chemistry of tourmaline, a detailed chemical characterization is recommended for a real distinction between these two species.

Formation of Ca,Fe-rich tourmalines (lucchesiite and feruvite) requires specific geochemical conditions that are rare in nature – high activity of Ca and Fe combined with rather low activity of Mg. Such conditions occur in some hydrothermal tourmaline and quartz-tourmaline veins (e.g. Grice and Robinson, 1989; Demirel *et al.*, 2009), exocontacts of highly evolved granitic pegmatites with mafic rocks (Selway *et al.*, 1998, 2000), and externally contaminated granitic pegmatites (e.g. Novák *et al.*, 2013*b*; Gadas *et al.*, 2014 and references therein). Data for published Ca,Fe-tourmaline compositions were reviewed recently by Gadas *et al.* (2014).

Despite the hydroxy- to oxy-species substitution feruvite → lucchesiite ($^{Z}Mg^{2+} + {}^{O1}(OH)^{1-} \rightarrow {}^{Z}Al^{3+} + {}^{O1}O^{2-}$), the mineral assemblage at Mirošov indicates that its formation is not constrained by oxidizing conditions. This is in agreement with

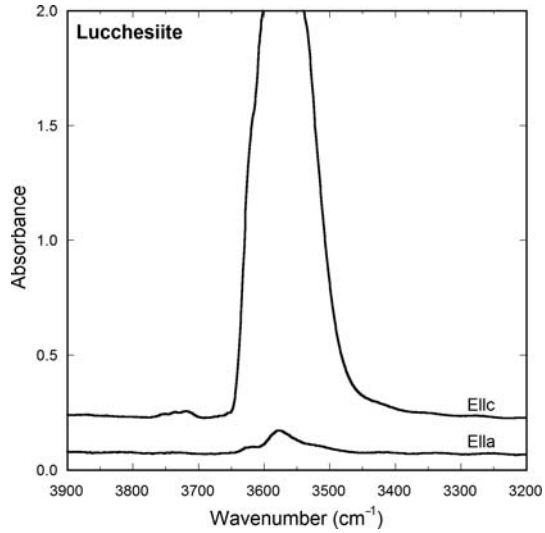


FIG. 3. Polarized FTIR spectra for lucchesiite from Sri Lanka. Note lack of significant bands above 3650 cm$^{-1}$. The main band is truncated at ~2 absorbance units in the **E**//**c** direction due to excessive absorption.

TABLE 9. Selected properties of lucchesiite and feruvite.

| | Lucchesiite | Feruvite |
|---|---|---|
| Formula | $CaFe_3Al_6(Si_6O_{18})(BO_3)_3(OH)_3O$ | $CaFe_3(Al_5Mg)(Si_6O_{18})(BO_3)_3(OH)_3(OH)$ |
| Space group | *R*3*m* | *R*3*m* |
| *a* (Å) | 16.0018(7) | 16.012(2) |
| *c* (Å) | 7.2149(3) | 7.245(2) |
| *V* (Å$^3$) | 1599.92(15) | 1606.6(4) |
| Optic sign | Uniaxial (–) | Uniaxial (–) |
| ω | 1.670(5) | 1.687(1) |
| ε | 1.655(5) | 1.669(1) |
| Colour | Black | Dark brown-black |
| Pleochroism | O = very dark brown<br>E = light brown | O = very dark brown[a]<br>E = light brown[a] |
| Reference | This study | Grice and Robinson (1989) |
| Geological environment | Contaminated pegmatites in Ca,Fe-rich host rocks | Contaminated pegmatites in Ca,Fe-rich host rocks<br>Pegmatite exocontacts with mafic rocks<br>Hydrothermal quartz-tourmaline veins |

[a] The pleochroism reported in Grice and Robinson (1989), O = light brown and E = very dark brown, is incorrect.; it should be reversed (J.D. Grice, 2015, pers comm.).

mineral assemblages of other aluminous oxy-species such as oxy-schorl (Bačík *et al.*, 2013), oxy-dravite (Bosi and Skogby 2013; Cempírek *et al.* 2013) or darrellhenryite (Novák *et al.*, 2013*a*). Instead, high activity of Al and low activity of F are essential for formation of aluminous oxy-species of the tourmaline-supergroup minerals.

## Acknowledgements

The authors appreciate constructive reviews by F.C. Hawthorne, R. Oberti, D. Henry and the Associate Editor I. Graham. Chemical analyses were undertaken with the kind assistance of M. Serracino to whom the authors express their gratitude. This work was

supported by the research project GAČR P210/14/13347S to PG, MN and JC. Funding by Sapienza University of Rome (Prog. Università 2015 to F.B.), the Swedish Research Council (H.S.) and the Ministry of Education, Youth and Sports of the Czech Republic (project LO1305) is gratefully acknowledged.

## References

Andreozzi, G.B., Bosi, F. and Longo, M. (2008) Linking Mössbauer and structural parameters in elbaite-schorl-dravite tourmalines. *American Mineralogist*, **93**, 658–666.

Bačík, P., Cempírek, J., Uher, P., Novák, M., Ozdín, D., Filip, J., Škoda, R., Breiter, K., Klementová, M. and Ďuďa, R. (2013) Oxy-schorl, $Na(Fe^{2+}_2Al)Al_6Si_6O_{18}(BO_3)_3(OH)_3O$, a new mineral from Zlatá Idka, Slovak Republic and Přibyslavice, Czech Republic. *American Mineralogist*, **98**, 485–492.

Bosi, F. (2010) Octahedrally coordinated vacancies in tourmaline: a theoretical approach. *Mineralogical Magazine*, **74**, 1037–1044.

Bosi, F. (2013) Bond-valence constraints around the O1 site of tourmaline. *Mineralogical Magazine*, **77**, 343–351.

Bosi, F. and Lucchesi, S. (2004) Crystal chemistry of the schorl-dravite series. *European Journal of Mineralogy*, **16**, 335–344.

Bosi, F. and Lucchesi, S. (2007) Crystal chemical relationships in the tourmaline group: structural constraints on chemical variability. *American Mineralogist*, **92**, 1054–1063.

Bosi, F. and Skogby, H. (2013) Oxy-dravite, $Na(Al_2Mg)(Al_5Mg)(Si_6O_{18})(BO_3)_3(OH)_3O$, a new mineral species of the tourmaline supergroup. *American Mineralogist*, **98**, 1442–1448.

Bosi, F., Balić-Žunić, T. and Surour, A.A. (2010) Crystal structure analysis of four tourmalines from the Cleopatra's Mines (Egypt) and Jabal Zalm (Saudi Arabia), and the role of Al in the tourmaline group. *American Mineralogist*, **95**, 510–518.

Bosi, F., Reznitskii, L. and Skogby, H. (2012*a*) Oxy-chromium-dravite, $NaCr_3(Cr_4Mg_2)(Si_6O_{18})(BO_3)_3(OH)_3O$, a new mineral species of the tourmaline supergroup. *American Mineralogist*, **97**, 2024–2030.

Bosi, F., Skogby, H., Agrosì, G. and Scandale, E. (2012*b*) Tsilaisite, $NaMn_3Al_6(Si_6O_{18})(BO_3)_3(OH)_3OH$, a new mineral species of the tourmaline supergroup from Grotta d'Oggi, San Pietro in Campo, island of Elba, Italy. *American Mineralogist*, **97**, 989–994.

Bosi, F., Reznitskii, L. and Sklyarov, E.V. (2013*a*) Oxy-vanadium-dravite, $NaV_3(V_4Mg_2)(Si_6O_{18})(BO_3)_3(OH)_3O$: crystal structure and redefinition of the 'vanadium-dravite' tourmaline. *American Mineralogist*, **98**, 501–505.

Bosi, F., Andreozzi, G.B., Skogby, H., Lussier, A.J., Abdu, Y. and Hawthorne, F.C. (2013*b*) Fluor-elbaite, $Na(Li_{1.5}Al_{1.5})Al_6(Si_6O_{18})(BO_3)_3(OH)_3F$, a new mineral species of the tourmaline supergroup. *American Mineralogist*, **98**, 297–303.

Bosi, F., Skogby, H., Reznitskii, L. and Hålenius, U. (2014*a*) Vanadio-oxy-dravite, $NaV_3(Al_4Mg_2)(Si_6O_{18})(BO_3)_3(OH)_3O$, a new mineral species of the tourmaline supergroup. *American Mineralogist*, **99**, 218–224.

Bosi, F., Reznitskii, L., Skogby, H. and Hålenius, U. (2014*b*) Vanadio-oxy-chromium-dravite, $NaV_3(Cr_4Mg_2)(Si_6O_{18})(BO_3)_3(OH)_3O$, a new mineral species of the tourmaline supergroup. *American Mineralogist*, **99**, 1155–1162.

Bosi, F., Andreozzi, G.B., Agrosì, G. and Scandale, E. (2015*a*) Fluor-tsilaisite, $NaMn_3Al_6(Si_6O_{18})(BO_3)_3(OH)_3F$, a new tourmaline from San Piero in Campo (Elba, Italy) and new data on tsilaisitic tourmaline from the holotype specimen locality. *Mineralogical Magazine*, **79**, 89–101.

Bosi, F., Andreozzi, G.B., Hålenius, U. and Skogby, H. (2015*b*) Experimental evidence for partial $Fe^{2+}$ disorder at the *Y* and *Z* sites of tourmaline: a combined EMP, SREF, MS, IR and OAS study of schorl. *Mineralogical Magazine*, **79**, 515–528.

Bosi, F., Skogby, H., Lazor, P., Reznitskii, L. (2015*c*) Atomic arrangements around the O3 site in Al- and Cr-rich oxy-tourmalines: a combined EMP, SREF, FTIR and Raman study. *Physics and Chemistry of Minerals*, **42**, 441–453.

Cempírek, J., Houzar, S., Novák, M., Groat, L.A., Selway, J.B. and Šrein, V. (2013) Crystal structure and compositional evolution of vanadium-rich oxy-dravite from graphite quartzite at Bítovánky, Czech Republic. *Journal of Geosciences*, **58**, 149–162.

Clark, C.M., Hawthorne, F.C. and Ottolini, L. (2011) Fluor-dravite, $NaMg_3Al_6Si_6O_{18}(BO_3)_3(OH)_3F$, a new mineral species of the tourmaline group from the Crabtree emerald mine, Mitchell County, North Carolina: description and crystal structure. *The Canadian Mineralogist*, **49**, 57–62.

Dahanayake, K. (1980) Modes of occurrence and provenance of gemstones of Sri Lanka. *Mineralium Deposita*, **15**, 81–86.

Demirel, S., Göncüoğlu, M.C., Topuz, G. and Isik, V. (2009) Geology and chemical variations in tourmaline from the quartz-tourmaline breccias within the Kerkenez granite-monzonite Massif, Central Anatolian Crystalline complex, Turkey. *The Canadian Mineralogist*, **47**, 787–799.

Dissanayake, C.B. and Rupasinghe, M.S. (1993) A prospectors' guide map to the gem deposits of Sri Lanka. *Gems and Gemology*, **29**, 173–181.

Ertl, A., Hughes, J.M., Pertlik, F., Foit, F.F. Jr., Wright, S.E., Brandstatter, F. and Marler, B. (2002) Polyhedron distortions in tourmaline. *The Canadian Mineralogist*, **40**, 153–162.

Ertl, A., Baksheev, I.A., Giester, G., Lengauer, C.L., Prokofiev, V.Yu. and Zorina, L.D. (2016*a*) Bosiite, $NaFe^{3+}_3(Al_4Mg_2)(Si_6O_{18})(BO_3)_3(OH)_3O$, a new ferric member of the tourmaline supergroup from the Darasun gold deposit, Transbaikalia, Russia. *European Journal of Mineralogy*, **28**, 581–591.

Ertl, A., Kolitsch, U., Dyar, M.D., Meyer, H.-P., Rossman, G.R., Henry, D.J., Prem, M., Ludwig, T., Nasdala, L., Lengauer, C.L., Tillmanns, E. and Niedemayr, G. (2016*b*) Fluor-schorl, a new member of the tourmaline supergroup, and new data on schorl from the cotype localities. *European Journal of Mineralogy*, **28**, 163–177.

Filip, J., Bosi, F., Novák, M., Skogby, H., Tuček, J., Čuda, J. and Wildner, M. (2012) Redox processes of iron in the tourmaline structure: example of the high-temperature treatment of $Fe^{3+}$-rich schorl. *Geochimica et Cosmochimica Acta*, **86**, 239–256.

Foit, F.F. Jr. (1989) Crystal chemistry of alkali-deficient schorl and tourmaline structural relationships. *American Mineralogist*, **74**, 422–431.

Gadas, P., Novák, M., Cempírek, J., Filip, J., Vašinová Galiová, M., Groat, L.A. and Všianský, D. (2014) Mineral assemblages, compositional variation, and crystal structure of feruvitic tourmaline from a contaminated anatectic pegmatite at Mirošov near Strážek, Moldanubian Zone, Czech Republic. *The Canadian Mineralogist*, **52**, 285–301.

Gebert, W. and Zemann, J. (1965) Messung des Ultrarot-Pleochroismus von Mineralen II. Der Pleochroismus der OH-Streckfrequenz in Turmalin. *Neues Jahrbuch für Mineralogie, Monatshefte*, **8**, 232–235.

Gonzales-Carreño, T., Fernández, M. and Sanz, J. (1988) Infrared and electron microprobe analysis of tourmaline. *Physics and Chemistry of Minerals*, **15**, 452–460.

Grice, J.D. and Ercit, T.S. (1993) Ordering of Fe and Mg in the tourmaline crystal structure: the correct formula. *Neues Jahrbuch für Mineralogie, Abhandlungen*, **165**, 245–266.

Grice, J.D. and Robinson, G.W. (1989) Feruvite, a new member of the tourmaline group, and its crystal structure. *The Canadian Mineralogist*, **27**, 199–203.

Hawthorne, F.C. (1996) Structural mechanisms for light-element variations in tourmaline. *The Canadian Mineralogist*, **34**, 123–132.

Hawthorne, F.C. (2002) Bond-valence constraints on the chemical composition of tourmaline. *The Canadian Mineralogist*, **40**, 789–797.

Hawthorne, F.C. and Henry, D. (1999) Classification of the minerals of the tourmaline group. *European Journal of Mineralogy*, **11**, 201–215.

Henry, D.J. and Dutrow, B.L. (2011) The incorporation of fluorine in tourmaline: Internal crystallographic controls or external environmental influences? *The Canadian Mineralogist*, **49**, 41–56.

Henry, D.J., Novák, M., Hawthorne, F.C., Ertl, A., Dutrow, B., Uher, P. and Pezzotta, F. (2011) Nomenclature of the tourmaline supergroup minerals. *American Mineralogist*, **96**, 895–913.

Herat, J.W. (1984) Geology and occurrence of gems in Sri Lanka. *Journal of Natural Sciences Council of Sri Lanka*, **12**, 257–271.

Holland, T.J.B. and Redfern, S.A.T. (1997) Unit cell refinement from powder diffraction data: the use of regression diagnostics. *Mineralogical Magazine*, **61**, 65–77.

Lussier, A.J., Ball, N.A., Hawthorne, F.C., Henry, D.J., Shimizu, R., Ogasawara, Y. and Ota, T. (2016) Maruyamaite, $K(MgAl_2)(Al_5Mg)Si_6O_{18}(BO_3)_3(OH)_3O$, from the ultrahigh-pressure Kokchetav massif, northern Kazakhstan: Description and crystal structure. *American Mineralogist*, **101**, 355–361.

Mandarino, J.A. (1981) The Gladstone-Dale relationship. Part IV: the compatibility concept and its application. *The Canadian Mineralogist*, **19**, 441–450.

Mendis, D.P.J., Rupasinghe, M.S. and Dissanayake, C.B. (1993) Application of structural geology in exploration for gem deposits of Sri Lanka. *Bulletin of Geological Society of Finland*, **65**, 31–40.

Munasinghe, T. and Dissanayake, C.B. (1981) The origin of gemstones in Sri Lanka. *Economic Geology*, **76**, 1216–1225.

Nishio-Hamane, D., Minakawa, T., Yamaura, J., Oyama, T., Ohnishi, M. and Shimobayashi, N. (2014) Adachiite, a Si–poor member of the tourmaline supergroup from the Kiura mine, Oita Prefecture, Japan. *Journal of Mineralogical and Petrological Sciences*, **109**, 74–78.

Novák, M., Povondra, P. and Selway, J.B. (2004) Schorl-oxy-schorl to dravite-oxydravite tourmaline from granitic pegmatites; examples from the Moldanubicum, Czech Republic. *European Journal of Mineralogy*, **16**, 323–333.

Novák, M., Škoda, R., Filip, J., Macek, I. and Vaculovič, T. (2011) Compositional trends in tourmaline from intragranitic NYF pegmatites of the Třebíč Pluton, Czech Republic; electron microprobe, Mössbauer and LA-ICP-MS study. *The Canadian Mineralogist*, **49**, 359–380.

Novák, M., Ertl, A., Povondra, P., Galiová, M.V., Rossman, G.R., Pristacz, H., Prem, M., Giester, G., Gadas, P. and Škoda, R. (2013*a*) Darrellhenryite, $Na(LiAl_2)Al_6(BO_3)_3Si_6O_{18}(OH)_3O$, a new mineral from the tourmaline supergroup. *American Mineralogist*, **98**, 1886–1892.

Novák, M., Kadlec, T. and Gadas, P. (2013*b*) Geological position, mineral assemblages and contamination of granitic pegmatites in the Moldanubian Zone, Czech Republic; examples from the Vlastějovice region. *Journal of Geosciences*, **58**, 21–47.

Pouchou, J.L. and Pichoir, F. (1991) Quantitative analysis of homogeneous or stratified microvolumes applying

the model "PAP." Pp. 3l–75 in: *Electron Probe Quantitation* (K.F.J. Heinrich and D.E. Newbury, editors). Plenum Press, New York.

Prescher, C., McCammon, C. and Dubrowinsky, L. (2012) *MossA*: a program for analyzing energy-domain Mössbauer spectra from conventional and synchrotron sources. *Journal of Applied Crystallography*, **45**, 329–331.

Reznitskii, L., Clark, C.M., Hawthorne, F.C., Grice, J.D., Skogby, H., Hålenius, U. and Bosi, F. (2014) Chromo-alumino-povondraite, $NaCr_3(Al_4Mg_2)(Si_6O_{18})(BO_3)_3$ $(OH)_3O$, a new mineral species of the tourmaline supergroup. *American Mineralogist*, **99**, 1767–1773.

Selway, J.B., Černý, P. and Hawthorne, F.C. (1998) Feruvite from lepidolite pegmatites at Red Cross Lake, Manitoba. *The Canadian Mineralogist*, **36**, 433–439.

Selway, J.B., Novák, M., Černý, P. and Hawthorne, F.C. (2000) The Tanco pegmatite at Bernic Lake, Manitoba. XIII. Exocontact tourmaline. *The Canadian Mineralogist*, **38**, 1095–1102.

Sheldrick, G.M. (2013) *SHELXL2013.* University of Göttingen, Germany.

Skogby, H., Bosi, F. and Lazor, P. (2012) Short-range order in tourmaline: a vibrational spectroscopic approach to elbaite. *Physics and Chemistry of Minerals*, **39**, 811–816.

Wright, S.E., Foley, J.A. and Hughes, J.M. (2000) Optimization of site occupancies in minerals using quadratic programming. *American Mineralogist*, **85**, 524–531.